Am J Transl Res 2025;17(8):5896-5913
www.ajtr.org /ISSN:1943-8141/AJTR0163523

Original Article

Decoding hub gene networks and miRNA interplay in Wilms tumor pathogenesis and therapeutic sensitivity

Weiwei Peng[1], Muhammad Haider[2], Salam Adil Ahmed[3], Rong Wang[1], Naeem ul Haq[4], Muhammad Sohaib Aslam[5], Majid Alhomrani[6,7], Ahmad A Alghamdi[8], Abdullah A Alqasem[9], Jamil A Samkari[10], Ahmed M Basri[11,12], Muhammad Jamil[13]

[1]School of Medicine and Pharmacy, Hunan Vocational College of Electronic and Technology, Changsha 410200, Hunan, China; [2]Department of Cardiology, Eastbourne District General Hospital, Eastbourne BN21 2YT, UK; [3]Department of Medical Laboratory Technology, Shaqlawa Technical College, Erbil Polytechnic University, Erbil, Iraq; [4]Department of Neurosurgery, Bacha khan Medical College/Mardan Medical Complex, KPK, Pakistan; [5]Department of Pathobiology, Riphah College of Veterinary Science, Riphah International University, Lahore 54000, Pakistan; [6]Department of Clinical Laboratories Sciences, The Faculty of Applied Medical Sciences, Taif University, Taif 21944, Saudi Arabia; [7]Research Centre for Health Sciences, Taif University, Taif 21944, Saudi Arabia; [8]Department of Clinical Laboratories Sciences, College of Applied Medical Sciences, Taif University, P.O. Box 11099, Taif 21944, Saudi Arabia; [9]Department of Medical Laboratory, College of Applied Medical Sciences, Prince Sattam bin Abdulaziz University, Al-Kharj 11942, Saudi Arabia; [10]Department of Family and Community Medicine, Faculty of Medicine, King Abdulaziz University, Rabigh 21589, Saudi Arabia; [11]Department of Medical Laboratory Sciences, Faculty of Applied Medical Sciences, King Abdulaziz University, Jeddah 21589, Saudi Arabia; [12]Embryonic Stem Cell Unit, King Fahd Medical Research Center, King Abdulaziz University, Jeddah 21589, Saudi Arabia; [13]PARC Arid Zone Research Centre, Dera Ismail Khan 29050, Pakistan

Received January 23, 2025; Accepted July 7, 2025; Epub August 15, 2025; Published August 30, 2025

Abstract: Objectives: This study aims to explore the expression and functional significance of hub genes in Wilms tumors and their potential as diagnostic biomarkers and therapeutic targets. Methods: Gene expression data from Wilms tumors and normal control samples were obtained from the Gene Expression Omnibus (GEO) database. Differentially expressed genes (DEGs) were identified using the limma package in R, followed by Venn diagram analysis to identify common DEGs. STRING and Cytoscape were employed to construct a protein-protein interaction (PPI) network and identify hub genes. Cell culture of five Wilms tumor cell lines and normal controls was performed to validate gene expression. Functional assays including proliferation, colony formation, and wound healing assays were conducted to assess the impact of SLC12A3 and GSTM3 overexpression. Immune infiltration analysis was carried out using ssGSEA. Results: We identified SLC12A3, CLCNKB, REN, and GSTM3 as hub genes with significant down-regulation across Wilms tumor cell lines and normal controls. Immune infiltration analysis revealed that the expression of these genes was associated with altered levels of immune cell populations, such as activated dendritic cells, CD8+ T cells, macrophages, and NK cells. GSTM3 overexpression enhanced the inflammatory response and reduced DNA damage, indicated by lower γ-H2AX expression. Functional assays showed that induction of SLC12A3 and GSTM3 overexpression significantly inhibited cell proliferation, colony formation, and migration. Conclusion: SLC12A3, CLCNKB, REN, and GSTM3 hub genes play key roles in regulating cellular functions and the immune microenvironment in Wilms tumors. Therefore, these genes could serve as potential biomarker and therapeutic targets in Wilms tumor patients.

Keywords: Wilms tumor, hub genes, biomarker, therapeutic target, prognosis

Introduction

Wilms tumor, also known as nephroblastoma, is a rare but aggressive form of kidney cancer that primarily affects children, typically under the age of five [1, 2]. It arises from immature kidney cells, and while it is a highly treatable disease when detected early, it can still result in significant morbidity and mortality [2]. Wilms tumor accounts for approximately 5-6% of all childhood cancers and remains the most common renal malignancy in children worldwide [3]. According to global cancer statistics, it is estimated that there are about 500 new cases

https://doi.org/10.62347/SLUH3891

annually in the United States alone, with varying prevalence across different regions [2].

Despite significant advances in treatment protocols over the past few decades, which include surgery, chemotherapy, and sometimes radiation, the survival rates for Wilms tumor are not optimal for all patients [1, 4, 5]. Particularly for those with advanced or relapsed disease, there is a critical need for novel, more effective therapeutic strategies [6]. Moreover, the identification of specific molecular biomarkers to aid in early diagnosis and to predict treatment responses remains an unmet need [7]. Although survival rates for early-stage Wilms tumor are high (around 90%), late-stage disease or relapse continues to be a major challenge in pediatric oncology [8].

The need for the study stems from the fact that while current diagnostic methods rely heavily on imaging and histopathological analysis, these techniques are not always sufficient for accurate prediction of disease progression, relapse, or response to therapy [9]. This highlights the critical importance of identifying biomarkers that can serve as both diagnostic markers and therapeutic targets. In recent years, genomic studies have identified various molecular signatures that could help in the early detection and personalized treatment of Wilms tumor [10]. However, the genetic landscape of Wilms tumor is still not completely understood, and its complex molecular mechanisms have not been fully explored. A major gap in the existing research is the lack of robust, universally applicable molecular biomarkers that could be integrated into clinical practice. Many studies have focused on identifying potential genes or pathways involved in Wilms tumor pathogenesis, but these findings have often been isolated or not fully validated using in vitro analysis [1, 11, 12]. Furthermore, the overlap of biomarkers identified in different studies remains unclear, and there is a lack of consensus on which molecular signatures are the most clinically relevant.

Several studies have previously attempted to uncover the genetic landscape of Wilms tumors using expression datasets and genomic analyses. For example, studies utilizing Gene Expression Omnibus (GEO) [13] datasets have identified potential biomarkers associated with disease progression and prognosis [9, 14-16]. However, many of these studies focus on single gene analysis or small datasets, which limits the generalizability of their findings [14, 15]. Other studies have investigated the role of specific signaling pathways, such as the Wnt/β-catenin and p53 pathways, in the pathogenesis of Wilms tumor [1, 17, 18]. Despite this, comprehensive studies identifying hub genes - genes that are central to the tumor network, often highly connected and involved in regulating critical pathways within the tumor microenvironment [19] - have been scarce. Identifying such hub genes could not only aid in diagnostic efforts but also provide new targets for therapeutic intervention. In this study, we aim to fill this gap by utilizing both public GEO expression datasets and in vitro analysis [20-22] to identify hub genes that may serve as reliable diagnostic markers and therapeutic targets in Wilms tumor patients.

Methodology

Data source and hub genes identification

In this study, we utilized different databases and tools to analyze differentially expressed genes (DEGs) and identify hub genes associated with Wilms tumor samples. The GEO database (https://www.ncbi.nlm.nih.gov/geo/) [13] provided the datasets GSE73209 and GSE11151, which contained gene expression profiles for Wilms tumor and normal control samples. The limma package in R (https://bioconductor.org/packages/release/bioc/html/limma.html) [23] was used for differential expression analysis to identify DEGs between the tumor and normal samples. Venn diagram [24] analysis was performed to identify common DEGs across both datasets, highlighting a shared molecular signature of Wilms tumor samples. To understand the biological relevance of these DEGs, the STRING database (https://string-db.org/) [24] was used to construct a protein-protein interaction (PPI) network, and Cytoscape (https://cytoscape.org/) (Version 3.1.9) was employed to visualize and analyze this network. The CutoHubba application within Cytoscape was then used to identify hub genes based on degree of centrality.

Cell culture

In this study, we purchased five Wilms tumor cell lines and five normal control cell lines to

investigate the expression and functional characterization of hub genes. The Wilms tumor cell lines included SIO-1, G401, SK-NEP-1, TC-71, and COV-504, while the normal control cell lines consisted of HEK 293T, HUVEC, WI-38, MCF-10A, and RPMI 1788. All cell lines were cultured in their respective growth media under standard conditions at 37°C and 5% CO_2. The Wilms tumor cell lines were cultured in RPMI-1640 medium supplemented with 10% fetal bovine serum (FBS), 1% penicillin-streptomycin, and 2 mM L-glutamine, while the normal control cell lines were cultured under different conditions. TC-71 cells were maintained in DMEM (Dulbecco's Modified Eagle Medium) supplemented with 10% FBS, 1% penicillin-streptomycin, and 2 mM L-glutamine, while HUVEC cells were cultured in Endothelial Cell Growth Medium-2 (EGM-2) containing specific growth factors for endothelial cells. WI-38 cells were cultured in EMEM (Eagle's Minimum Essential Medium) supplemented with 10% FBS and 1% penicillin-streptomycin. MCF-10A cells were maintained in DMEM/F12 medium supplemented with 5% horse serum, 20 ng/mL epidermal growth factor (EGF), 0.5 µg/mL hydrocortisone, 100 ng/mL cholera toxin, and 10 µg/mL insulin. RPMI 1788 cells were cultured in RPMI-1640 medium supplemented with 10% FBS and 1% penicillin-streptomycin. All cell lines were grown in a humidified incubator, with media changes every 2-3 days, and cells were subcultured upon reaching 70-80% confluence.

Reverse transcription quantitative polymerase chain reaction (RT-qPCR) analysis

Total RNA was extracted from the Wilms tumor and normal control cell lines using the RNAeasy Plus Mini Kit (Qiagen, Germany) according to the manufacturer's instructions. The RNA concentration and purity were assessed using a NanoDrop 2000 spectrophotometer (Thermo Fisher Scientific, USA), and only RNA samples with an A260/A280 ratio between 1.8 and 2.0 were used for further analysis. For reverse transcription, High-Capacity cDNA Reverse Transcription Kit (Thermo Fisher Scientific, USA) was used to synthesize complementary DNA (cDNA) from 1 µg of total RNA.

RT-qPCR was performed using SYBR Green Master Mix (Thermo Fisher Scientific, USA) on a QuantStudio 3 Real-Time PCR System (Thermo Fisher Scientific, USA). Each PCR reaction was carried out in a 20 µL final volume, containing 10 µL of SYBR Green Master Mix, 0.5 µM of forward and reverse primers, and 2 µL of cDNA. The housekeeping gene GAPDH was used as an internal control for normalization of gene expression. Relative expression levels of target genes (SLC12A3, REN, CLCNKB, and GSTM3) were calculated using the $2^{(-\Delta\Delta Ct)}$ method. All experiments were performed in triplicate, and the results are expressed as the mean ± standard deviation. Following primers were used for amplification purposes.

SLC12A3: Forward: 5'-TGGACGACCATTTCCTACCTGG-3', Reverse: 5'-CACTCGGTGAAGTTCCAGCCAT-3'; CLCNKB: Forward: 5'-CCCTCTACAAGACCAGTTTCCG-3', Reverse: 5'-GCTGACAGAAGAGGTAAGCGCT-3'; REN: Forward: 5'-GAAGAGG CTGACACTTGGCAAC-3', Reverse: 5'-GCACCCAAACATTGGACGAACC-3'; GSTM3: Forward: 5'-CGAAGCCAATGGCTGGATGTGA-3', Reverse: 5'-GTTGTGCTTGCGAGCGATGTAG-3'; H2AX: Forward: 5'-CGGCAGTGCTGGAGTACCTCA-3', Reverse: 5'-AGCTCCTCGTCGTTGCGGATG-3'; IFNG: Forward: 5'-GAGTGTGGAGACCATCAAGGAAG-3', Reverse: 5'-TGCTTTGCGTTGGACATTCAAGTC-3'; IL6: Forward: 5'-AGACAGCCACTCACCTCTTCAG-3', Reverse: 5'-TTCTGCCAGTGCCTCTTTGCTG-3'; TNF: Forward: 5'-CTCTTCTGCCTGCTGCACTTTG-3', Reverse: 5'-ATGGGCTACAGGCTTGTCACTC-3'; GAPDH: Forward: 5'-GTCTCCTCTGACTTCAACAGCG-3', Reverse: 5'-ACCACCCTGTTGCTGTAGCCAA-3'.

Prognostic significance of the hub genes

To assess the prognostic relevance of hub genes in Wilms tumor patients, we employed the "survival" package in R 3.5.2 software to conduct the log-rank test and Kaplan-Meier survival analysis. The Kaplan-Meier method, a widely used nonparametric tool in cancer survival studies, offers a reliable statistical approach for examining survival time. In this analysis, patients were divided into two groups based on the expression levels of each gene (high vs. low). The Kaplan-Meier survival estimates were calculated, and the corresponding survival curves were plotted for further interpretation.

Immune infiltration analysis of the hub genes

The immune infiltration levels were assessed using the single-sample Gene Set Enrichment

Analysis (ssGSEA) algorithm [25]. This analysis was based on 28 predefined immune-related gene sets to evaluate the extent of immune cell infiltration in the samples. The ssGSEA algorithm provides a score for each gene set in each sample, reflecting the relative enrichment of the gene set, which is used to infer the immune infiltration degree within the samples.

miRNA-mRNA network construction

A miRNA-mRNA network of the hub genes was constructed using the miRNet database (https://www.mirnet.ca/) [26] to investigate the potential regulatory interactions between miRNAs and hub genes in Wilms tumors. The miRNet database is a comprehensive resource for the prediction and analysis of miRNA-target interactions, integrating experimentally validated and computationally predicted miRNA-target pairs.

RT-qPCR analysis of hsa-mir-16-5p and hsa-mir-200c-3p was performed using TaqMan Universal PCR Master Mix (Thermo Fisher Scientific, USA) and TaqMan miRNA assays (Thermo Fisher Scientific, USA) specific to hsa-mir-16-5p and hsa-mir-200c-3p, following the manufacturer's instructions. The amplification was carried out in a QuantStudio 3 Real-Time PCR System (Thermo Fisher Scientific, USA). For normalization, the expression levels of hsa-mir-16-5p and hsa-mir-200c-3p were normalized to the expression of U6 small nuclear RNA (U6 snRNA), which was used as an internal control. The relative expression levels were calculated using the $2^{(-\Delta\Delta Ct)}$ method [27].

Gene enrichment analysis

Gene enrichment analysis of the hub genes SLC12A3, CLCNKB, REN, and GSTM3 was performed using the DAVID Bioinformatics Resources (https://david.ncifcrf.gov/) [28, 29], which is a comprehensive tool designed for functional annotation and enrichment analysis of gene lists. This tool helps in identifying the most relevant biological processes, molecular functions, and cellular components associated with a set of genes.

Pan-cancer expression and drug sensitivity analysis

To analyze the expression patterns of hub genes SLC12A3, CLCNKB, REN, and GSTM3 across various cancer types, we utilized the TIMER2.0 database (https://cistrome.shinyapps.io/timer/) [30]. The TIMER2.0 database is an online tool for the analysis of immune infiltration and gene expression across different cancer types using data from The Cancer Genome Atlas (TCGA). To assess the potential drug sensitivity of these hub genes, drug sensitivity analysis was performed using the GSCA database (https://www.bio-x.cn/GSCA) [31]. The analysis focused on the correlation between hub gene expression and the half-maximal inhibitory concentration (IC50) values of various chemotherapeutic agents obtained from the GDSC (Genomics of Drug Sensitivity in Cancer) database.

Overexpression of SLC12A3 and GSTM3

The SLC12A3 and GSTM3 genes were cloned into the pcDNA3.1 expression vectors (Thermo Fisher Scientific, USA), and the recombinant plasmids were confirmed by sequencing. The TC-71 cells were transfected with these expression vectors using Lipofectamine 3000 transfection reagent (Thermo Fisher Scientific, USA), following the manufacturer's protocol. Briefly, 2 μg of the plasmid DNA was mixed with Lipofectamine 3000 reagent and incubated with the cells for 6 hours in Opti-MEM medium (Gibco, Thermo Fisher Scientific, USA). After transfection, the medium was replaced with complete RPMI-1640 medium, and cells were cultured for 48-72 hours to allow for the overexpression of the target genes. Control cells were transfected with an empty vector (pcDNA3.1) under the same conditions. Successful transfection and overexpression of SLC12A3 and GSTM3 were confirmed by RT-qPCR and Western blotting (Thermo Fisher Scientific, USA), as described in previous methodologies.

Cell proliferation assay (CCK-8)

Cell proliferation was assessed using the Cell Counting Kit-8 (CCK-8) assay (Dojindo Laboratories, Japan). After transfection, TC-71 cells were seeded in a 96-well plate at a density of 1 × 10^4 cells per well and incubated for 24, 48, 72, and 96 hours. At each time point, 10 μL of CCK-8 solution was added to each well, and cells were incubated for 1 hour at 37°C. The absorbance at 450 nm was measured using a microplate reader (BioTek Instruments, USA).

The cell proliferation rate was calculated by comparing the absorbance values of the overexpression groups with the control cells.

Colony formation assay

To evaluate the clonogenic potential of SLC12A3 and GSTM3 overexpressing cells, a colony formation assay was performed. Following transfection, TC-71 cells were seeded at a low density of 500 cells per well in a 6-well plate and cultured in complete RPMI-1640 medium for 10-14 days, allowing the cells to form colonies. The colonies were fixed with 4% paraformaldehyde for 15 minutes and stained with crystal violet (Sigma-Aldrich, USA) for 30 minutes. The number of colonies (defined as > 40 cells) was counted under a light microscope (Olympus, Japan). The assay was performed in triplicate for each condition.

Wound healing assay

To assess the migratory ability of SLC12A3 and GSTM3 overexpressing TC-71 cells, a wound healing assay was performed. Transfected cells were cultured in a 6-well plate until they reached confluence. A linear scratch wound was created in the cell monolayer using a sterile 10 µL micropipette tip. The cells were then washed with PBS to remove detached cells and cultured in serum-free RPMI-1640 medium. Images of the wound were taken at 0 hours and 24 hours using a light microscope (Olympus, Japan). The wound closure was quantified by measuring the width of the wound at both time points using ImageJ software (National Institutes of Health, USA). The migration rate was calculated as the percentage of wound closure relative to the initial wound width.

Statistical analysis

All experiments were performed in triplicate, and data are presented as the mean ± standard deviation (SD). Statistical significance was assessed using Student's t-test for comparisons between two groups or one-way analysis of variance (ANOVA) followed by Tukey's post hoc test for comparisons among multiple groups. A p-value < 0.05 was considered statistically significant. Colony formation and wound healing assays were quantified by counting colonies and measuring wound closure, respectively, using ImageJ software. All statistical analyses were performed using GraphPad Prism (version 8.0, GraphPad Software, USA).

Results

Datasets acquisition and hub gene identification

Two expression datasets (GSE73209 and GSE11151) from the GEO database, corresponding to Wilms tumor and normal control samples, were analyzed to identify differentially expressed genes (DEGs) using the limma package in R. The analysis revealed a substantial number of DEGs between the Wilms tumor and normal control samples, with the majority of the genes exhibiting significant changes in expression levels (**Figure 1A**, **1B**). Further investigation through a Venn diagram analysis (**Figure 1C**) of the GSE73209 dataset revealed that 504 genes were commonly differentially expressed in both GSE73209 and GSE11151, while 160 genes were shared across both datasets, signifying a common molecular signature of Wilms tumor (**Figure 1C**). The common DEGs from both datasets were subjected to a PPI network construction using the STRING database and Cytoscape software was used to analyze the PPI network (**Figure 1D**). Using CutoHubba application of Cytoscape software, four hub genes, including SLC12A3, REN, CLCNKB, and GSTM3 were revealed based on the higher degree of centrality (**Figure 1D**).

Expression analysis and diagnostic performance of hub genes

The expression of the hub genes SLC12A3, REN, CLCNKB, and GSTMT3 was validated using RT-qPCR across five Wilms tumor cell lines and five normal control cell lines. The results showed significant (P^{***}-value < 0.001) down-regulation of all four genes in the Wilms tumor samples compared to normal controls (**Figure 2A**). Next, ROC curve analysis was performed on the RT-qPCR data, yielding AUC values of 0.54 for SLC12A3, 0.58 for REN, 0.50 for CLCNKB, and 0.57 for GSTMT3 (**Figure 2B**). Further validation was conducted using the GSE11024 dataset, which showed consistent down-regulation of SLC12A3, REN, CLCNKB, and GSTMT3 in Wilms tumor samples compared to normal controls (**Figure 2C**). ROC curve analysis using the GSE11024 dataset yielded higher AUC values: 0.94 for SLC12A3, 0.75 for REN, 0.72 for CLCNKB, and 0.77 for GSTMT3 (**Figure 2D**). These higher AUC values indicate that these genes show strong diagnostic poten-

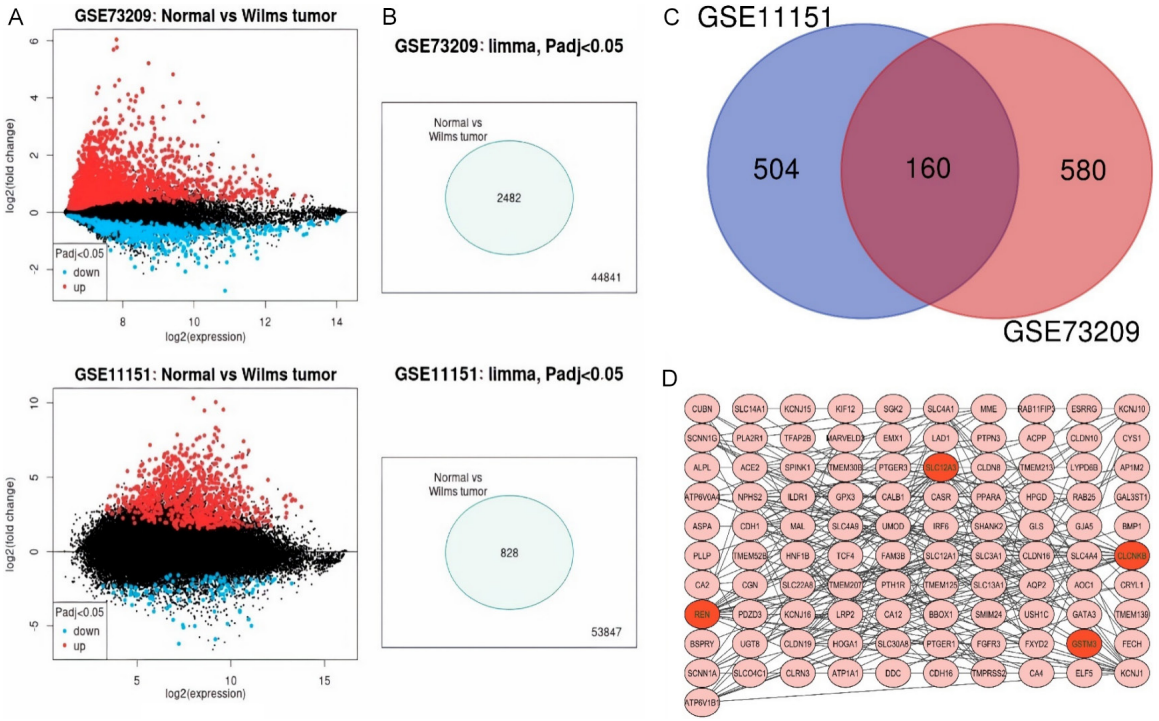

Figure 1. Identification of Differentially Expressed Genes (DEGs) and hub genes in Wilms tumor samples. A, B. Differential expression analysis of Wilms tumor and normal control samples from two Gene Expression Omnibus (GEO) datasets (GSE73209 and GSE11151) using the limma package in R. C. Venn diagram analysis of the GSE73209 and GSE11151, with 160 shared DEGs across both datasets. D. Protein-protein interaction (PPI) network constructed using the STRING database and visualized in Cytoscape, with four hub genes (SLC12A3, REN, CLCNKB, and GSTM3) identified based on the highest degree of centrality using the CutoHubba application.

tial demonstrating excellent discriminatory ability between Wilms tumor and normal samples.

Prognostic and immune infiltration analysis of hub genes

The Wilms tumor patients were categorized into two groups based on the median expression levels of each of the hub genes: SLC12A3, REN, CLCNKB, and GSTM3. Kaplan-Meier survival curves were generated for each gene, and a log-rank test was applied to compare the survival differences between the high-expression and low-expression groups. The analysis revealed statistically significant differences in survival times between the two groups for all four genes, including SLC12A3, REN, CLCNKB, and GSTM3. The survival probability for Wilms tumor patients with lower expression levels of SLC12A3, REN, CLCNKB, and GSTM3 was noticeably lower compared to those with high expression (**Figure 3A**).

To further explore the biological implications of these hub genes, immune infiltration analysis was performed using the single-sample gene set enrichment analysis (ssGSEA) algorithm (**Figure 3B**). The results demonstrated distinct differences in immune cell infiltration levels between the normal and Wilms tumor groups for each gene. Notably, the expression of SLC12A3, REN, CLCNKB, and GSTM3 was associated with altered levels of several immune cell populations, including activated dendritic cells (aDCs), CD8+ T cells, macrophages, and natural killer (NK) cells (**Figure 3B**). Many immune cell types exhibited statistically significant differences ($P < 0.01$) between the groups, indicating that these hub genes may be involved in modulating the tumor immune microenvironment.

miRNA-mRNA network analysis

A miRNA-mRNA network of hub genes was constructed using the miRNet database (**Figure 4A**). In this network, miRNAs that target all four hub genes simultaneously were identified as crucial. Specifically, two miRNAs (hsa-mir-16-

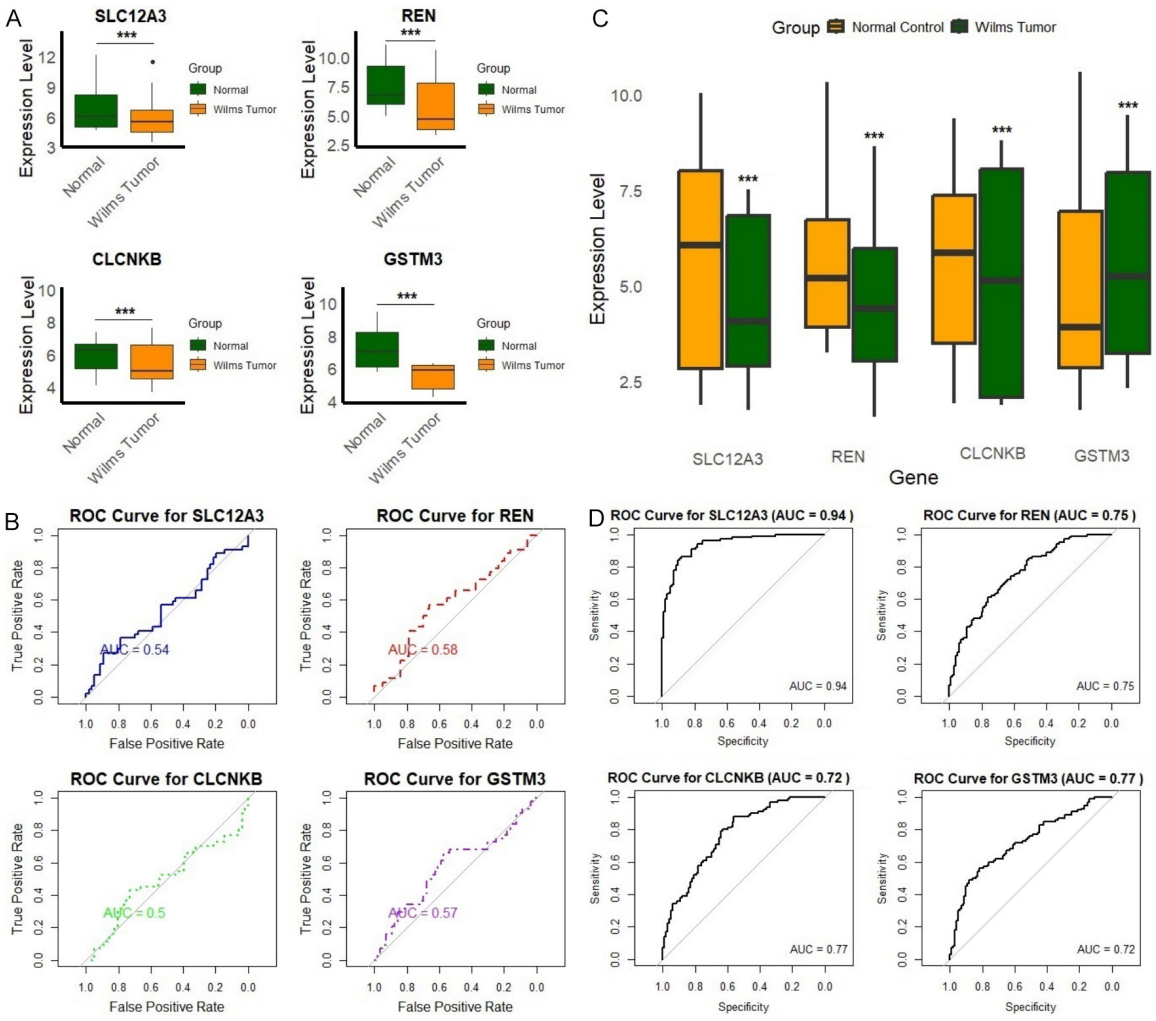

Figure 2. Expression analysis and diagnostic performance of hub genes in Wilms tumors. A. Reverse transcription quantitative polymerase chain reaction (RT-qPCR) validation of hub gene expression (SLC12A3, REN, CLCNKB, and GSTM3) across five Wilms tumor cell lines and five normal control cell lines. B. Receiver operating characteristic (ROC) curve analysis of RT-qPCR data. C. Expression validation using the GSE11024 dataset. D. ROC curve analysis of hub genes using data from the GSE11024 dataset. *P****-value < 0.001.

5p and hsa-mir-200c-3p) were found to be particularly significant due to their ability to regulate all four hub genes, namely GST3M, SLC12A3, CLCNKB, and REN (**Figure 4A**). The expression of the two identified key miRNAs was evaluated across five Wilms tumor cell lines and five normal control cell lines via RT-qPCR. The results illustrated that hsa-mir-16-5p and hsa-mir-200c-3p miRNAs exhibited higher expression in the Wilms tumor cell lines in tumor samples compared to the normal controls (**Figure 4B**). The ROC curves for these two miRNAs were generated based on RT-qPCR data. The ROC curve for hsa-mir-16-5p and hsa-mir-200c-3p showed AUC of 0.840 and 0.928, indicating a good ability to differentiate between Wilms tumor patients and normal individuals (**Figure 4C**).

Gene enrichment analysis

Gene enrichment analysis of hub genes (SLC12A3, CLCNKB, REN, and GST3M) was performed using the DAVID tool. The enrichment analysis of cellular component terms revealed two key components with significant enrichment: “Sperm fibrous sheath and Chloride channel complex (**Figure 5A**)”. In the molecular function category, the most enriched terms included “Glutathione binding, Voltage-gated chloride channel activity, Insulin-like growth factor receptor binding, and Oligopeptide bind-

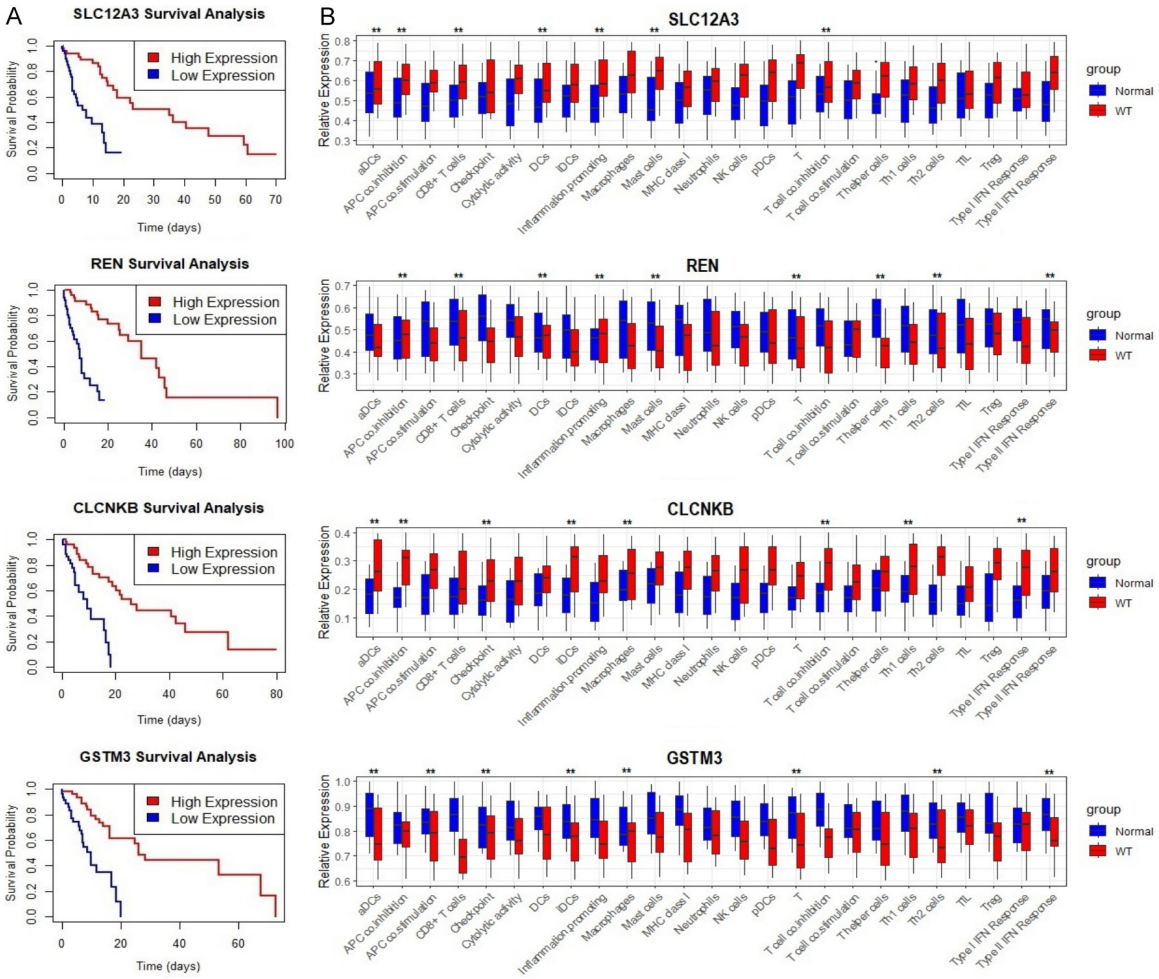

Figure 3. Prognostic and immune infiltration analysis of hub genes in Wilms tumors. A. Kaplan-Meier survival curves were generated for each of the hub genes (SLC12A3, REN, CLCNKB, and GSTM3) based on median expression levels. B. Immune infiltration analysis of Wilms tumor patients using the single-sample Gene Set Enrichment Analysis (ssGSEA) algorithm. *P***-value < 0.01.

ing (**Figure 5B**)". The biological processes that were most strongly enriched included terms related to "Renin-angiotensin regulation of aldosterone production, Renal sodium ion transport, Angiotensin maturation, and Regulation of blood volume by renin-angiotensin (**Figure 5C**)". In the KEGG pathways analysis, the most enriched terms were associated with the "Renin-angiotensin system, Glutathione metabolism, and Drug metabolism by cytochrome P450 (**Figure 5D**)".

Pan-cancer expression and drug sensitivity analysis

The expression patterns of the hub genes SLC12A3, CLCNKB, REN, and GSTM3 were analyzed across pan-cancer using the TIMER2.0 database. Notably, all four genes demonstrated significant differential expression across multiple cancer types (indicated by asterisks, P < 0.05, P < 0.01, P < 0.001). Specifically, SLC12A3 exhibited under expression in KIRC and KIRP, while showing overexpression in cancers like LUAD and UCEC, etc. (**Figure 6A**). Similarly, CLCNKB was significantly downregulated in multiple cancers including LUAD, and LUSC etc. (**Figure 6A**), but upregulated in a few such as BRCA and KICH etc. (**Figure 6A**). REN showed significantly high expression in kidney-related tumors including KICH and KIRP etc. (**Figure 6A**). GSTM3 displayed both upregulation and downregulation across various tumor types, with notable overexpression in PCPG and low expression in PAAD and READ (**Figure 6A**). Concerning clinical significance, the differential

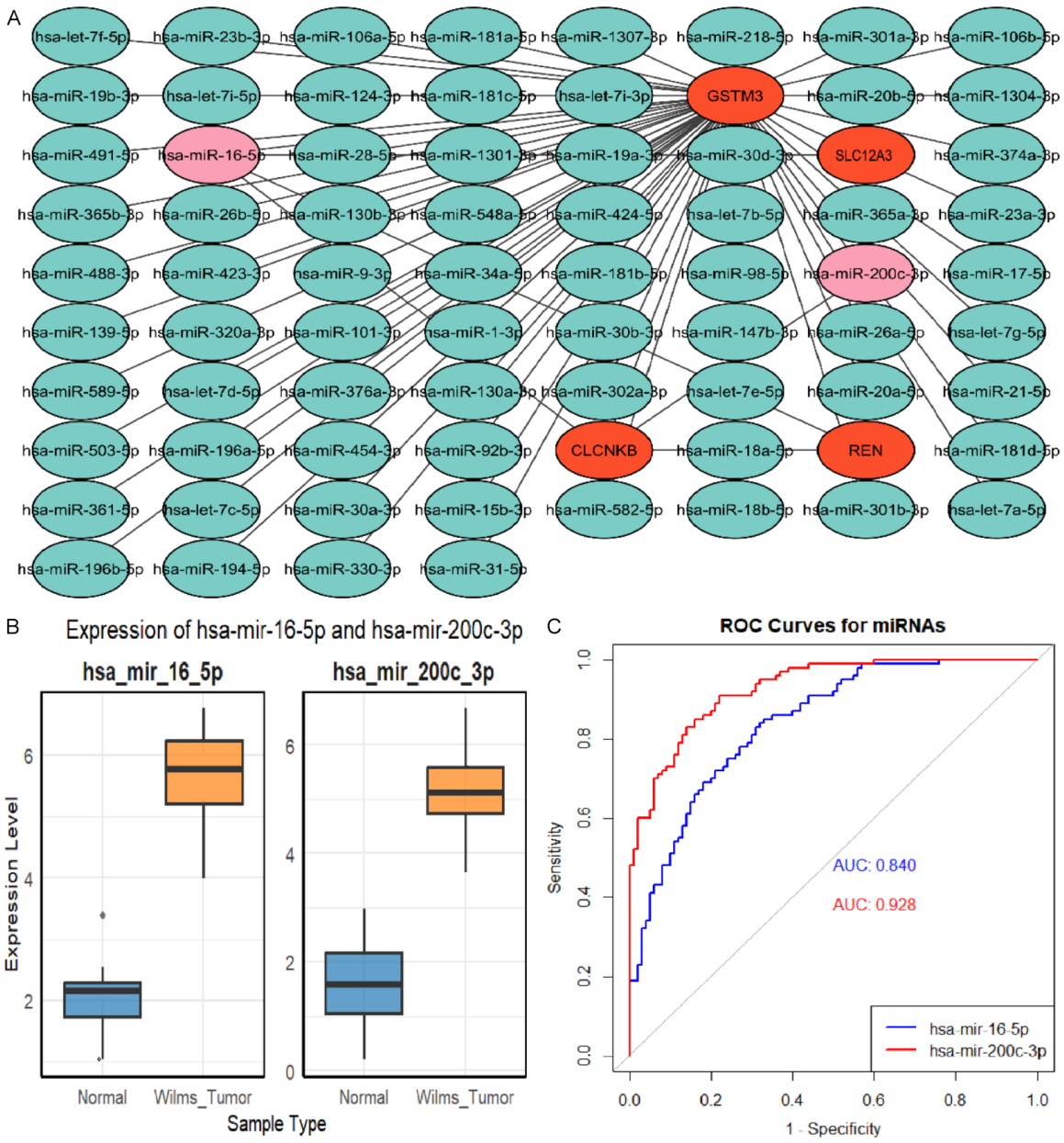

Figure 4. miRNA-mRNA network analysis and diagnostic performance of miRNAs in Wilms Tumors. A. miRNA-mRNA network of hub genes (SLC12A3, REN, CLCNKB, and GSTM3) constructed using the miRNet database. B. Reverse transcription quantitative polymerase chain reaction (RT-qPCR) analysis of the expression levels of hsa-mir-16-5p and hsa-mir-200c-3p across five Wilms tumor cell lines and five normal control cell lines. C. Receiver operating characteristic (ROC) curve analysis of hsa-mir-16-5p and hsa-mir-200c-3p miRNAs. *P*-value < 0.05.

expression patterns of SLC12A3, CLCNKB, REN, and GSTM3 across various cancer types suggest that these genes have significant potential as pan-cancer biomarkers. Their ability to distinguish between different tumor types and their association with key aspects of cancer progression, such as immune response modulation, tumor aggressiveness, and treatment resistance, positions them as promising candidates for early detection, prognosis prediction, and therapeutic targeting in diverse cancers. Drug sensitivity analysis of the hub genes was conducted using the GSCA database, focusing on their correlation with the half-maximal inhibitory concentration (IC50) of various chemotherapeutic agents from the GDSC database. Significant drug resistance (positive correlation with IC50; red circles) was obser-

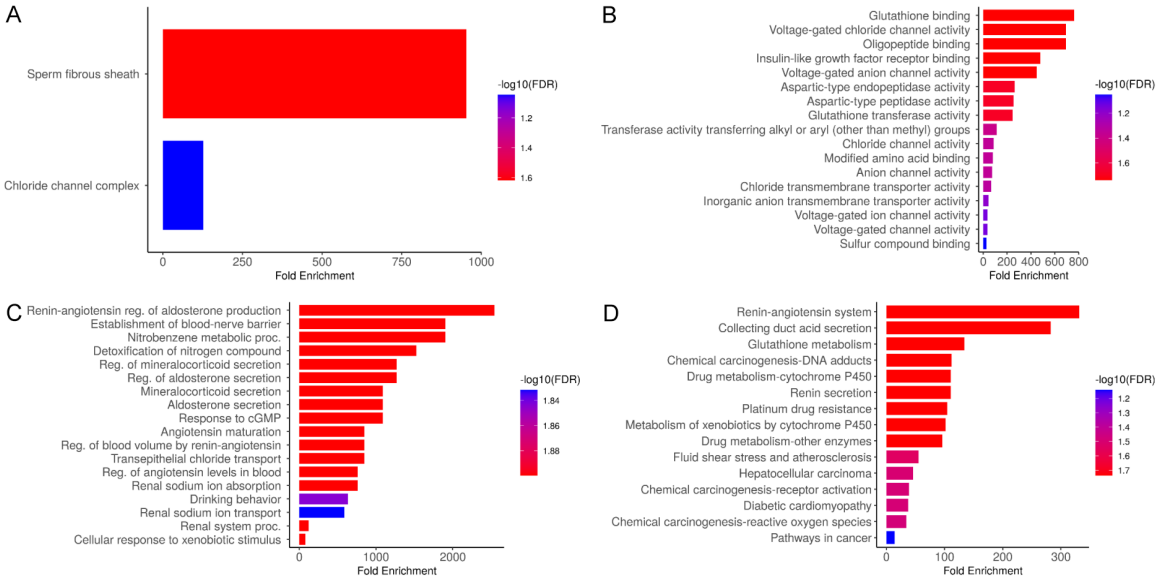

Figure 5. Gene enrichment analysis of hub genes in Wilms tumors using the DAVID tool. A. Enrichment analysis of cellular component terms. B. Molecular function enrichment analysis. C. Biological process enrichment analysis. D. Kyoto Encyclopedia of Genes and Genomes (KEGG) pathway enrichment analysis. *P*-value < 0.05.

ved for CLCNKB, REN, and GSTM3 across several agents. Notably, CLCNKB expression was strongly and significantly associated with resistance to agents such as bleomycin, Docetaxel, and 17-AAG (**Figure 6B**). GSTM3 also exhibited significant resistance associations, particularly with I-BET-762 and BIX02189 (**Figure 6B**). REN expression correlated positively with resistance to multiple agents, including AR-42 and BIX02189 (**Figure 6B**).

Functional characterization of SLC12A3 and GSTM3 overexpression in TC-71 cells

To investigate the potential roles of SLC12A3 and GSTM3 in regulating cellular phenotypes, we performed functional assays following their overexpression in TC-71 cells. As shown in **Figure 7A**, quantitative RT-PCR confirmed that SLC12A3 mRNA levels were significantly elevated in TC-71 cells transfected with the SL-C12A3 expression vector compared to control cells (P < 0.001). This overexpression was further validated at the protein level by Western blotting (**Figures 7B** and S1), demonstrating increased SLC12A3 protein expression. Functionally, overexpression of SLC12A3 markedly suppressed cellular proliferation, as quantified by a proliferation assay (**Figure 7C**), where the OE-SLC-12A3-TC-71 cells exhibited significantly reduced proliferation rates compared to controls (P < 0.001). Colony formation assays revealed a notable decline in colony numbers in the SLC12A3-overexpressing cells (**Figure 7D**, **7E**), indicating impaired clonogenic potential (P < 0.001). In addition, wound healing assays demonstrated that SLC12A3 overexpression significantly inhibited cell migratory ability (**Figure 7F**, **7G**). Quantification of wound closure percentage (**Figure 7F**) and representative micrographs at 0 h and 24 h (**Figure 7G**) confirmed the reduced migratory capacity of OESLC12A3-TC-71 cells relative to controls (P < 0.001). Similarly, we assessed the biological impact of GSTM3 overexpression in TC-71 cells. RT-qPCR analysis demonstrated significant upregulation of GSTM3 mRNA levels in the overexpression group compared to controls (P < 0.001; **Figure 8A**), which was corroborated by Western blot analysis showing enhanced GSTM3 protein expression (**Figures 8B** and S1). Consistent with the SLC12A3 data, GSTM3 overexpression significantly inhibited cell proliferation (**Figure 8C**), reduced colony formation capacity (**Figure 8D**, **8E**), and decreased cell migration (**Figure 8F**, **8G**) compared to the control group (P < 0.001 for all assays).

To investigate the role of GSTM3 in modulating the immune response, the expression of genes coding for inflammatory cytokines such as IL-6, TNF-α, and IFN-γ was analyzed in Ctrl-GSTM3-

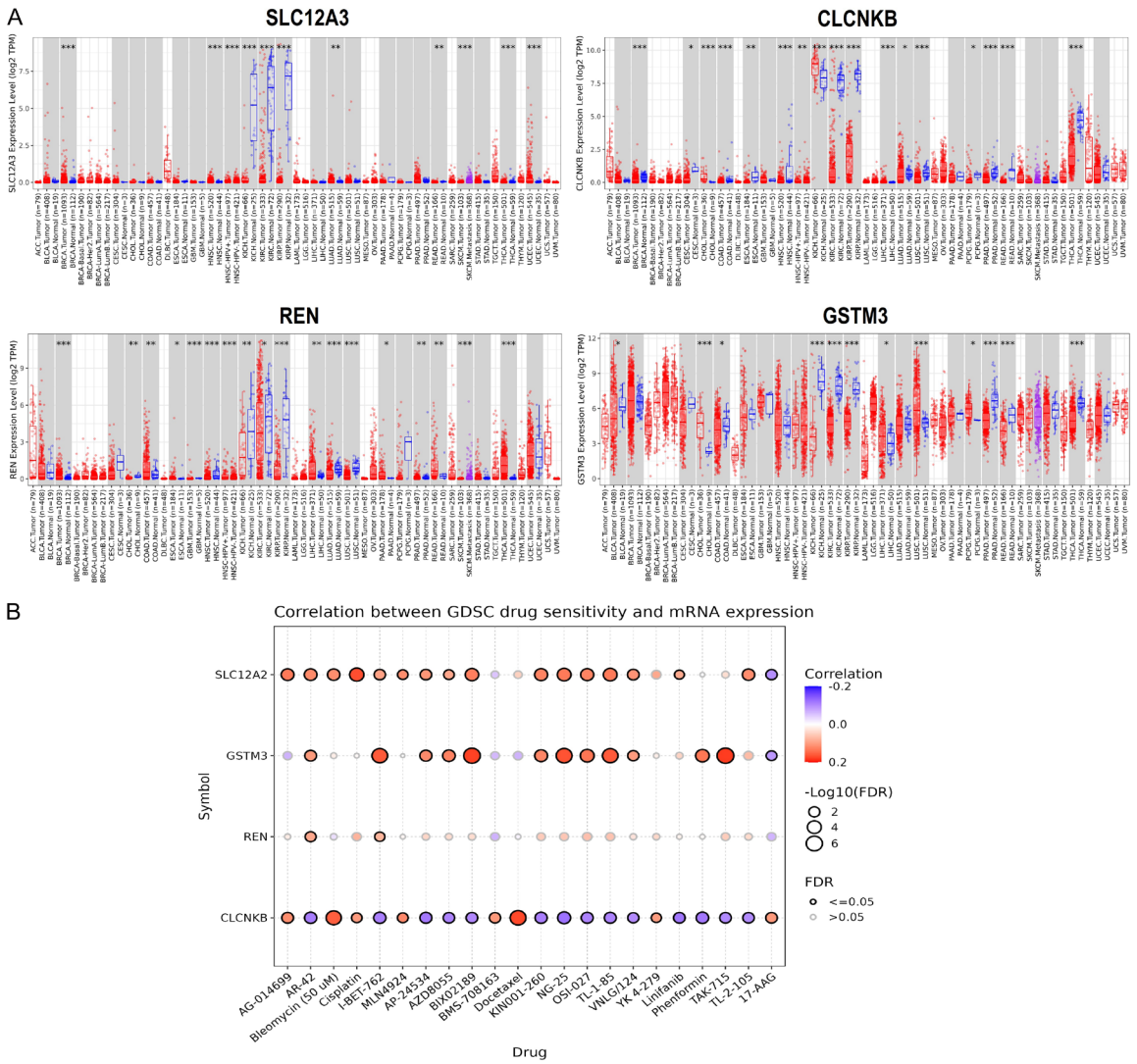

Figure 6. Pan-cancer expression and drug sensitivity analysis of hub genes. A. Expression patterns of hub genes (SLC12A3, CLCNKB, REN, and GSTM3) across multiple cancer types analyzed using the TIMER2.0 database. B. Drug sensitivity analysis of hub genes using the GSCA database. *P**-value < 0.05, *P***-value < 0.01, and *P****-value < 0.001.

TC-71 and OE-GSTM3-TC-71 cells via RT-qPCR (**Figure 8H**). The expression levels of these genes were significantly higher in OE-GSTM3-TC-71 cells compared to Ctrl-GSTM3-TC-71 cells. These results suggest that GSTM3 overexpression enhances the inflammatory response in Wilms tumor cells, potentially through the regulation of pro-inflammatory cytokines, which could influence the immune microenvironment (**Figure 8H**). Furthermore, to explore the potential mechanism through which GSTM3 regulates genome stability, we analyzed the expression of the gene which encodes for DNA damage marker γ-H2AX. The expression of γ-H2AX, a marker of DNA double-strand breaks, was significantly lower in GSTM3 overexpressed cells, indicating lower levels of DNA damage (**Figure 8H**).

Discussion

Wilms tumor, a pediatric renal malignancy, is the most common type of kidney cancer in children [8, 32]. It typically presents in early childhood and, despite advances in treatment, remains a significant cause of morbidity and mortality [33]. Despite its high cure rate with appropriate treatment, the molecular mechanisms

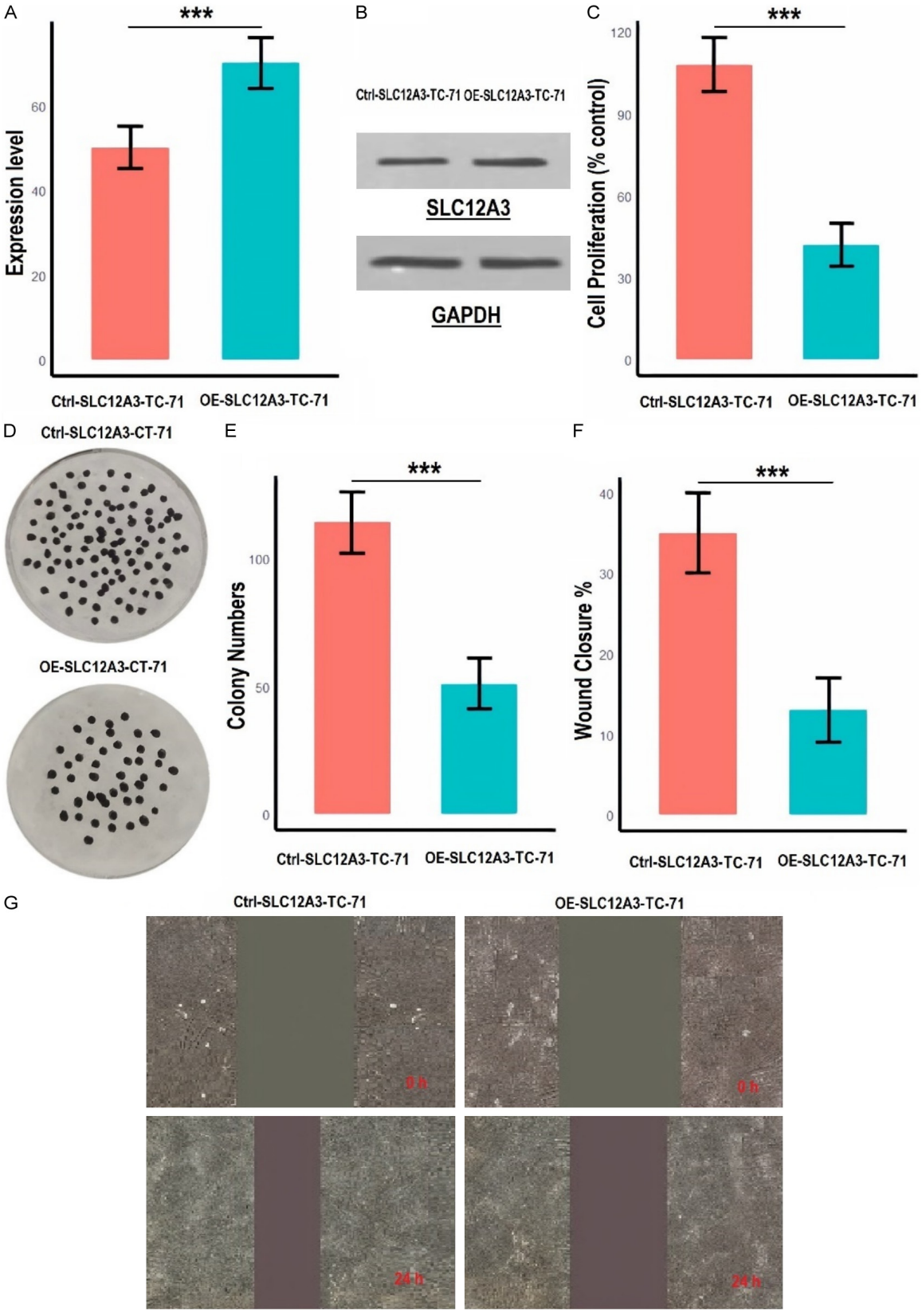

Figure 7. Functional characterization of SLC12A3 overexpression in TC-71 cells. (A) Reverse transcription quantitative polymerase chain reaction (RT-qPCR) analysis showing significant upregulation of SLC12A3 mRNA levels in TC-71 cells transfected with the SLC12A3 expression vector compared to control cells. (B) Western blot analysis confirming increased SLC12A3 protein expression in TC-71 cells. (C) Proliferation assay demonstrates significantly

reduced proliferation rates in SLC12A3-overexpressing TC-71 cells. (D, E) Colony formation assay showing a notable decline in colony numbers in SLC12A3-overexpressing cells, indicating impaired clonogenic potential. (F, G) Wound healing assay demonstrating significantly reduced cell migration in SLC12A3-overexpressing cells, with quantification of wound closure percentage (F) and representative micrographs at 0 h and 24 h (G), confirming impaired migratory capacity. *P****-value < 0.001.

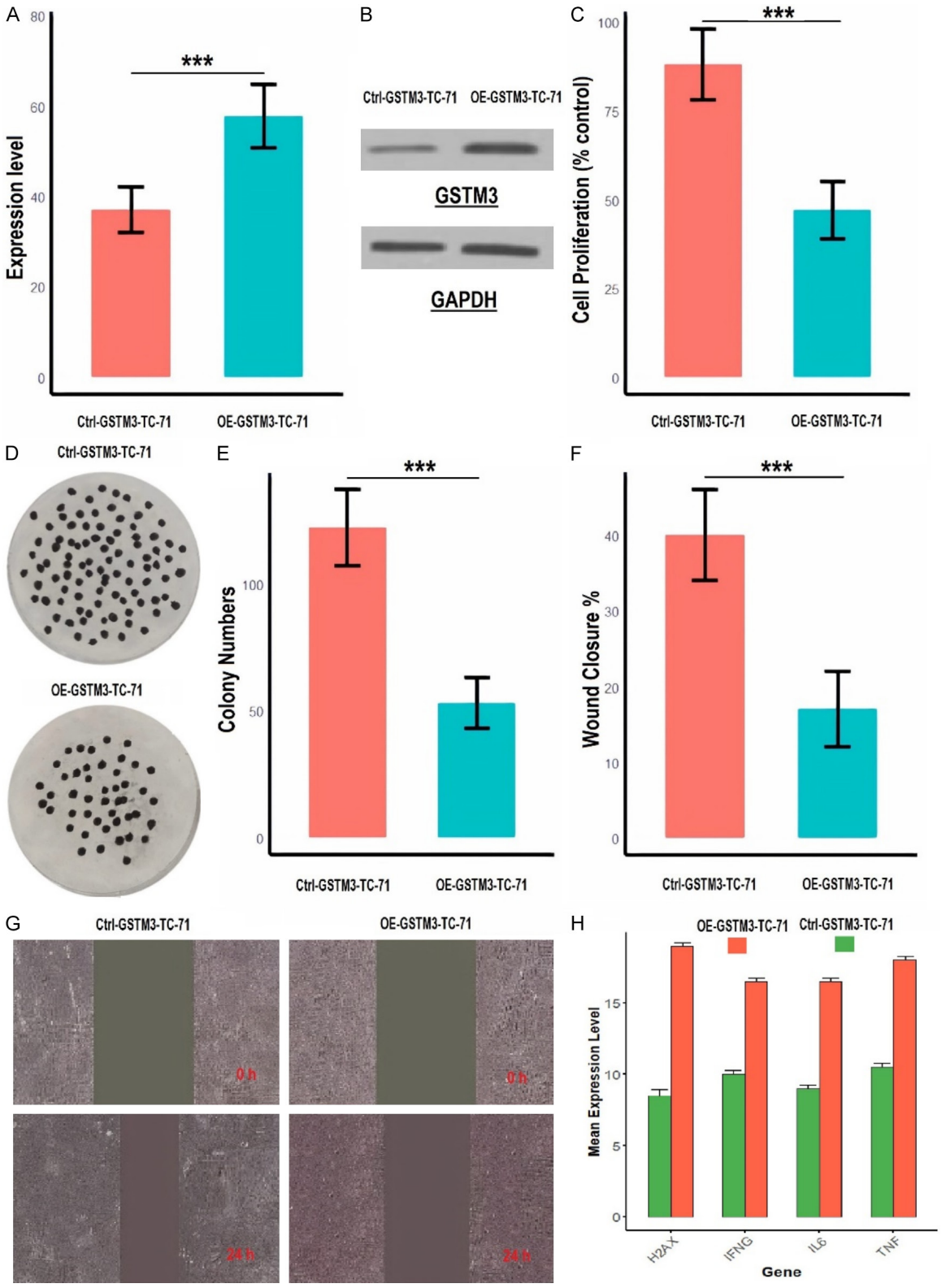

Figure 8. Functional characterization of GSTM3 overexpression in TC-71 cells. (A) Reverse transcription quantitative polymerase chain reaction (RT-qPCR) analysis showing significant upregulation of GSTM3 mRNA levels in TC-71 cells transfected with the GSTM3 expression vector compared to control cells. (B) Western blot analysis confirming enhanced GSTM3 protein expression in GSTM3-overexpressing TC-71 cells. (C) Proliferation assay demonstrating significant inhibition of cell proliferation in GSTM3-overexpressing TC-71 cells (OE-GSTM3) compared to control cells. (D, E) Colony formation assay showing reduced colony formation in GSTM3-overexpressing cells, indicating impaired clonogenic potential. (F, G) Wound healing assay showing decreased cell migration in GSTM3-overexpressing cells, with quantification of wound closure percentage (F) and representative micrographs (G) showing significant reduction in migration. (H) Expression analysis of inflammatory cytokines (IL-6, TNF-α, IFN-γ) and γ-H2AX, a marker for DNA double-strand breaks, in Ctrl-GSTM3-TC-71 and OE-GSTM3-TC-71 cells via RT-qPCR. *P***-value < 0.05 and *P****-value < 0.001.

underpinning Wilms tumors remain poorly understood, and there is a continued need for the identification of robust biomarkers for diagnosis and prognosis, as well as therapeutic targets [33, 34]. Recent studies have identified genetic alterations, signaling pathways, and miRNAs associated with Wilms tumor [35], but a comprehensive understanding of the molecular signature of this disease is still lacking. A critical gap exists in the ability to identify reliable diagnostic and prognostic markers [36, 37], as well as understanding the therapeutic implications [38] of these molecular changes.

This study aimed to address these gaps by identifying and validating hub genes associated with Wilms tumor samples. Through the acquisition of gene expression data from two datasets (GSE73209 and GSE11151), differential expression analysis was conducted to pinpoint key genes implicated in Wilms tumors. Additionally, we investigated the prognostic significance of these genes, the potential regulatory role of miRNAs, and performed functional characterization of selected genes.

Several previous studies have identified genes related to Wilms tumors. For example, the role of WT1 (Wilms Tumor 1 gene) has been extensively studied due to its pivotal role in kidney development and its frequent mutations in Wilms tumor patients [1, 39]. In the previous literature, gene expression analyses and their relation to clinical outcomes in Wilms tumor have been explored to some extent. For example, work by Qi et al. examined the expression of WT1 and its relationship to survival, but these studies were more focused on single-gene analysis [40]. Another key study by Phelps et al. identified IGF2 as a potential prognostic biomarker in Wilms tumor, reporting that lower levels of IGF2 expression were associated with poor survival outcomes [41]. Our study builds on these findings by including a panel of hub genes (SLC12A3, REN, CLCNKB, and GSTM3) and providing statistical evidence for their prognostic value. This extends the findings from earlier studies that emphasized the importance of individual genes by considering the collective impact of multiple genes within a network context [42-44].

Although previous studies have utilized miRNA-mRNA network analysis in cancer research [45, 46], the application of this approach to Wilms tumors is relatively novel. In particular, while previous studies, such as those by Kheiry et al. have identified individual miRNAs involved in cancer progression [47], our study uniquely highlights the role of miRNAs (hsa-mir-16-5p and hsa-mir-200c-3p) in regulating a network of hub genes in Wilms tumors. The high AUC values for these miRNAs in the ROC curve analysis suggest their potential as diagnostic biomarkers, which is a significant advancement over previous studies that have not integrated miRNA regulatory networks to this extent.

The immune infiltration analysis of SLC12A3, REN, CLCNKB, and GSTM3 using the ssGSEA algorithm revealed significant differences in immune cell populations between the normal and Wilms tumor groups, with altered infiltration levels of key immune cells, including activated dendritic cells (aDCs), CD8+ T cells, macrophages, and natural killer (NK) cells. These findings are consistent with previous studies suggesting that the tumor immune microenvironment plays a crucial role in cancer progression and response to treatment [48-50]. For instance, elevated CD8+ T cell and NK cell infiltration has been linked to improved anti-tumor immunity in various cancers [51, 52], while the presence of macrophages and dendritic cells often reflects a more immunosuppressive environment, contributing to tumor progression and immune evasion [51, 53]. The observed changes in immune cell infiltration associated with

SLC12A3, REN, CLCNKB, and GSTM3 are in line with studies that have reported that genes influencing the immune landscape can modulate tumor behavior and therapeutic responses [54, 55]. Specifically, studies on GSTM3 have highlighted its potential in regulating oxidative stress and immune responses [56, 57], while SLC12A3 and CLCNKB have been implicated in influencing the tumor immune microenvironment in other cancers, such as breast and lung cancer [58, 59]. These results suggest that the hub genes identified in our study may not only serve as biomarkers for Wilms tumors but could also represent novel targets for therapeutic strategies aimed at modulating immune cell infiltration and enhancing anti-tumor immunity.

While this study provides valuable insights into the molecular mechanisms and prognostic potential of hub genes in Wilms tumors, a few limitations should be considered. Firstly, the study relies on publicly available datasets (GSE73209, GSE11151, and GSE11024), which may have inherent biases and variations due to differences in sample collection, processing, and patient demographics, potentially affecting the generalizability of the findings. Secondly, although we validated the expression of hub genes using RT-qPCR across multiple cell lines, the findings were not corroborated by clinical tissue samples, which would have added more clinical relevance to our conclusions. Additionally, while we performed functional assays on TC-71 cells to investigate the biological impact of gene overexpression, these results may not fully represent the complex tumor microenvironment in vivo. These limitations emphasize the need for future studies involving clinical samples and in vivo models to validate and extend our findings.

Conclusion

In summary, our study provides new insights into the molecular underpinnings of Wilms tumor by identifying and validating hub genes, revealing their prognostic significance, and uncovering their regulation by specific miRNAs. The novel use of PPI network analysis, miRNA-mRNA interaction studies, and functional validation of gene expression offers a comprehensive view of the molecular landscape of Wilms tumors. These findings pave the way for the development of more accurate diagnostic tools, prognostic markers, and potential therapeutic strategies targeting the identified hub genes and miRNAs.

Acknowledgements

The authors extend their appreciation to Taif University, Saudi Arabia, for supporting this work through project number (TU-DSPP-2024-15). This research was funded by Taif University, Saudi Arabia, Project No. (TU-DSPP-2024-15).

Disclosure of conflict of interest

None.

Address correspondence to: Muhammad Jamil, PARC Arid Zone Research Centre, Dera Ismail Khan 29050, Pakistan. E-mail: Jamilmatrah@parc.gov.pk; Rong Wang, School of Medicine and Pharmacy, Hunan Vocational College of Electronic and Technology, Changsha 410200, Hunan, China. E-mail: wangrong1605@163.com; Naeem ul Haq, Department of Neurosurgery, Bacha khan Medical College/Mardan Medical Complex, KPK, Pakistan. E-mail: Brainsurgeon1978@yahoo.com; Muhammad Sohaib Aslam, Department of Pathobiology, Riphah College of Veterinary Science, Riphah International University, Lahore 54000, Pakistan. E-mail: sohaib.aslam@riphah.edu.pk

References

[1] Neagu MC, David VL, Iacob ER, Chiriac SD, Muntean FL and Boia ES. Wilms' tumor: a review of clinical characteristics, treatment advances, and research opportunities. Medicina (Kaunas) 2025; 61: 491.

[2] Perotti D, O'Sullivan MJ, Walz AL, Davick J, Al-Saadi R, Benedetti DJ, Brzezinski J, Ciceri S, Cost NG, Dome JS, Drost J, Evageliou N, Furtwängler R, Graf N, Maschietto M, Mullen EA, Murphy AJ, Ortiz MV, van der Beek JN, Verschuur A, Wegert J, Williams R, Spreafico F, Geller JI, van den Heuvel-Eibrink MM and Hong AL. Hallmark discoveries in the biology of non-Wilms tumour childhood kidney cancers. Nat Rev Urol 2025; 23: 1-18.

[3] Pio L, Bruno T, Godzinski J, Ehrlich PF, Cost N, Davidoff AM, Irtan S, Pachl M, Abu-Zaid A, Abdelhafeez AH and Losty PD. Comparison of open and minimally invasive nephrectomy for Wilms tumor: a systematic review and meta-analysis from the International Society of Pediatric Surgical Oncology. Pediatr Surg Int 2025; 41: 117.

[4] Reddy DBAKS, Pagare C, Suman HWKPS, Panda S, Chandra KSKPK and Barot V. Metabolic pathways in Wilms Tumour: Implications for

therapies and paradigm shift in treatment. 2025.
[5] Zhou Y, Li Q, Pan R, Wang Q, Zhu X, Yuan C, Cai F, Gao YD and Cui Y. Regulatory roles of three miRNAs on allergen mRNA expression in tyrophagus putrescentiae. Allergy 2022; 77: 469-482.
[6] Khan MS, Maaz AUR, Qazi AQ, Aslam S, Riaz S, Malik AS and Shaheen N. Prognostic impact of pre-referral tumor resection in unilateral Wilms tumor: a single-institute experience from a lower middle-income country. Pediatr Blood Cancer 2024; 71: e30760.
[7] Sahu DK, Singh N, Das M, Rawat J and Gupta DK. Differential expression profiling of onco and tumor-suppressor genes from major-signaling pathways in Wilms' tumor. Pediatr Surg Int 2022; 38: 1601-1617.
[8] Cui K, Hong P, Lin J, Hu Z, Gao Z, Tian X, Lin T, Shi Q and Wei G. Hope and challenges in the diagnosis and treatment of Wilms tumor: a single-center retrospective study in China. Front Pediatr 2025; 13: 1527039.
[9] Cai L, Shi B, Zhu K, Zhong X, Lai D, Wang J and Tou J. Bioinformatical analysis of the key differentially expressed genes for screening potential biomarkers in Wilms tumor. Sci Rep 2023; 13: 15404.
[10] Ding C, Li G, Li Y, Gao H and Sun F. The construction and experimental verification of a 6-LncRNA model based on Lactic acid metabolism in the tumor microenvironment of Wilms tumor. Gene 2025; 932: 148898.
[11] Bitaraf M, Mahmanzar M, Zafari N, Mohammadpour H, Vasei M, Moradi Matin L, Kajbafzadeh AM and Majidi Zolbin M. The potential key genes and pathways associated with Wilms tumor in quest of proper candidates for diagnostic and therapeutic purposes. Sci Rep 2022; 12: 17906.
[12] Karam S, Gebreil A, Alksas A, Balaha HM, Khalil A, Ghazal M, Contractor S and El-Baz A. Insights into personalized care strategies for Wilms tumor: a narrative literature review. Biomedicines 2024; 12: 1455.
[13] Clough E and Barrett T. The gene expression omnibus database. Methods Mol Biol 2016; 1418: 93-110.
[14] Wang Y, Gao H, Li X, Li D, Huang F, Sun Y, Liu X, Yang J and Sun F. PRC1 as an independent adverse prognostic factor in Wilms tumor via integrated bioinformatics and experimental validation. Sci Rep 2025; 15: 13282.
[15] Wang X, Li X, Tan L, Zhang F, Zhang J, Zhao X, Zhang Y, Du G and Liu W. Identification and validation of lipid metabolism gene FASN-associated miRNA in Wilms tumor. Biochem Genet 2025; 63: 167-182.
[16] Jiang F, Ahmad S, Kanwal S, Hameed Y and Tang Q. Key wound healing genes as diagnostic biomarkers and therapeutic targets in uterine corpus endometrial carcinoma: an integrated in silico and in vitro study. Hereditas 2025; 162: 5.
[17] Perotti D, Hohenstein P, Bongarzone I, Maschietto M, Weeks M, Radice P and Pritchard-Jones K. Is Wilms tumor a candidate neoplasia for treatment with WNT/β-catenin pathway modulators?-A report from the renal tumors biology-driven drug development workshop. Mol Cancer Ther 2013; 12: 2619-2627.
[18] Li H, Hohenstein P and Kuure S. Embryonic kidney development, stem cells and the origin of Wilms tumor. Genes (Basel) 2021; 12: 318.
[19] Ekman D, Light S, Björklund ÅK and Elofsson A. What properties characterize the hub proteins of the protein-protein interaction network of Saccharomyces cerevisiae? Genome Biol 2006; 7: R45.
[20] Qian FC, Zhou LW, Li YY, Yu ZM, Li LD, Wang YZ, Xu MC, Wang QY and Li CQ. SEanalysis 2.0: a comprehensive super-enhancer regulatory network analysis tool for human and mouse. Nucleic Acids Res 2023; 51: W520-W527.
[21] Yang Z, Liu X, Xu H, Teschendorff AE, Xu L, Li J, Fu M, Liu J, Zhou H, Wang Y, Zhang L, He Y, Lv K and Yang H. Integrative analysis of genomic and epigenomic regulation reveals miRNA mediated tumor heterogeneity and immune evasion in lower grade glioma. Commun Biol 2024; 7: 824.
[22] Yang H, Zhou H, Fu M, Xu H, Huang H, Zhong M, Zhang M, Hua W, Lv K and Zhu G. TMEM64 aggravates the malignant phenotype of glioma by activating the Wnt/β-catenin signaling pathway. Int J Biol Macromol 2024; 260: 129332.
[23] Ni J, Huang K, Xu J, Lu Q and Chen C. Novel biomarkers identified by weighted gene co-expression network analysis for atherosclerosis. Herz 2024; 49: 198-209.
[24] Pelikan A, Herzel H, Kramer A and Ananthasubramaniam B. Venn diagram analysis overestimates the extent of circadian rhythm reprogramming. FEBS J 2022; 289: 6605-6621.
[25] Huang L, Wu C, Xu D, Cui Y and Tang J. Screening of important factors in the early sepsis stage based on the evaluation of ssGSEA algorithm and ceRNA regulatory network. Evol Bioinform Online 2021; 17: 11769343211058463.
[26] Chang L, Zhou G, Soufan O and Xia J. miRNet 2.0: network-based visual analytics for miRNA functional analysis and systems biology. Nucleic Acids Res 2020; 48: W244-W251.
[27] Huang L, Irshad S, Sultana U, Ali S, Jamil A, Zubair A, Sultan R, Abdel-Maksoud MA, Mubarak A, Almunqedhi BM, Almanaa TN, Malik A, Alamri A, Kodous AS, Mares M, Zaky MY,

Saba Sajjad S and Hameed Y. Pan-cancer analysis of HS6ST2: associations with prognosis, tumor immunity, and drug resistance. Am J Transl Res 2024; 16: 873-888.
[28] Franz M, Rodriguez H, Lopes C, Zuberi K, Montojo J, Bader GD and Morris Q. GeneMANIA update 2018. Nucleic Acids Res 2018; 46: W60-W64.
[29] Abdel-Maksoud MA, Ullah S, Nadeem A, Shaikh A, Zia MK, Zakri AM, Almanaa TN, Alfuraydi AA, Mubarak A and Hameed Y. Unlocking the diagnostic, prognostic roles, and immune implications of BAX gene expression in pan-cancer analysis. Am J Transl Res 2024; 16: 63-74.
[30] Li T, Fu J, Zeng Z, Cohen D, Li J, Chen Q, Li B and Liu XS. TIMER2.0 for analysis of tumor-infiltrating immune cells. Nucleic Acids Res 2020; 48: W509-W514.
[31] Liu CJ, Hu FF, Xie GY, Miao YR, Li XW, Zeng Y and Guo AY. GSCA: an integrated platform for gene set cancer analysis at genomic, pharmacogenomic and immunogenomic levels. Brief Bioinform 2023; 24: bbac558.
[32] Trinder S, Kiraly-Borri C, Dholaria H, Charles A, Roebuck D and Ryan A. Renal masses in childhood: an Australian perspective. J Paediatr Child Health 2025; 27: 21-26.
[33] Salzillo C, Cazzato G, Serio G and Marzullo A. Paediatric renal tumors: a state-of-the-art review. Curr Oncol Rep 2025; 27: 211-214.
[34] Feng C, Wang Y, Xu J, Zheng Y, Zhou W, Wang Y and Luo C. Precisely tailoring molecular structure of doxorubicin prodrugs to enable stable nanoassembly, rapid activation, and potent antitumor effect. Pharmaceutics 2024; 16: 1582.
[35] Alfaifi J. miRNAs role in Wilms tumor pathogenesis: signaling pathways interplay. Pathol Res Pract 2024; 256: 155254.
[36] Satturwar S and Parwani AV. Cytomorphology of papillary renal neoplasm with reverse polarity. Cytojournal 2023; 20: 43.
[37] Guo Z, Guan K, Bao M, He B and Lu J. LINC-PINT plays an anti-tumor role in nasopharyngeal carcinoma by binding to XRCC6 and affecting its function. Pathol Res Pract 2024; 260: 155460.
[38] Yu QY, Meng M, Yao JF, Du SS and Qi YK. Two step synthesis of octreotide-doxorubicin conjugates based on disulfide bond linker. Acta Chimica Sinica 2025; 83: 341-353.
[39] Lu J, Zhang X, Liu H and Liu Y. Exploring the multifaceted role of WT1 in kidney development and disease. Kidney Blood Press Res 2025; 50: 176-188.
[40] Qi XW, Zhang F, Wu H, Liu JL, Zong BG, Xu C and Jiang J. Wilms' tumor 1 (WT1) expression and prognosis in solid cancer patients: a systematic review and meta-analysis. Sci Rep 2015; 5: 8924.
[41] Phelps HM, Kaviany S, Borinstein SC and Lovvorn HN 3rd. Biological drivers of Wilms tumor prognosis and treatment. Children (Basel) 2018; 5: 145.
[42] Li J, Zhang Y, Shu W, Feng X, Wang Y, Yan P, Li X, Sha C and He M. M4: multi-proxy multi-gate mixture of experts network for multiple instance learning in histopathology image analysis. Med Image Anal 2025; 103: 103561.
[43] Hu H, Umair M, Khan SA, Sani AI, Iqbal S, Khalid F, Sultan R, Abdel-Maksoud MA, Mubarak A, Dawoud TM, Malik A, Saleh IA, Al Amri AA, Algarzae NK, Kodous AS and Hameed Y. CDCA8, a mitosis-related gene, as a prospective pan-cancer biomarker: implications for survival prognosis and oncogenic immunology. Am J Transl Res 2024; 16: 432-445.
[44] Wu X, Fu M, Ge C, Zhou H, Huang H, Zhong M, Zhang M, Xu H, Zhu G, Hua W, Lv K and Yang H. m6A-mediated upregulation of lncRNA CHASERR promotes the progression of glioma by modulating the miR-6893-3p/TRIM14 axis. Mol Neurobiol 2024; 61: 5418-5440.
[45] Hu M, Yuan X, Liu Y, Tang S, Miao J, Zhou Q and Chen S. IL-1β-induced NF-κB activation downregulates miR-506 expression to promotes osteosarcoma cell growth through JAG1. Biomed Pharmacother 2017; 95: 1147-1155.
[46] Lin X, Yu T, Zhang L, Chen S, Chen X, Liao Y, Long D and Shen F. Silencing Op18/stathmin by RNA interference promotes the sensitivity of nasopharyngeal carcinoma cells to taxol and high-grade differentiation of xenografted tumours in nude mice. Basic Clin Pharmacol Toxicol 2016; 119: 611-620.
[47] Kheiry M and Maleki F. Role of the microRNA in prediction of the breast cancer. J Basic Res Med Sci 2025; 12: 54-61.
[48] Ahmad M, Khan M, Asif R, Sial N, Abid U, Shamim T, Hameed Z, Iqbal MJ, Sarfraz U and Saeed H. Expression characteristics and significant diagnostic and prognostic values of ANLN in human cancers. Int J Gen Med 2022; 15: 1957-1972.
[49] Sial N, Rehman JU, Saeed S, Ahmad M, Hameed Y, Atif M, Rehman A, Asif R, Ahmed H, Hussain MS, Khan MR, Ambreen A and Ambreen A. Integrative analysis reveals methylenetetrahydrofolate dehydrogenase 1-like as an independent shared diagnostic and prognostic biomarker in five different human cancers. Biosci Rep 2022; 42: BSR20211783.
[50] Cao Z, Zhu J, Wang Z, Peng Y and Zeng L. Comprehensive pan-cancer analysis reveals ENC1 as a promising prognostic biomarker for tumor microenvironment and therapeutic responses. Sci Rep 2024; 14: 25331.

[51] Lin Y, Song Y, Zhang Y, Li X, Kan L and Han S. New insights on anti-tumor immunity of CD8+ T cells: cancer stem cells, tumor immune microenvironment and immunotherapy. J Transl Med 2025; 23: 341.
[52] Sun DY, Hu YJ, Li X, Peng J, Dai ZJ and Wang S. Unlocking the full potential of memory T cells in adoptive T cell therapy for hematologic malignancies. Int Immunopharmacol 2025; 144: 113392.
[53] Hameed Y and Ejaz S. TP53 lacks tetramerization and N-terminal domains due to novel inactivating mutations detected in leukemia patients. J Cancer Res Ther 2021; 17: 931-937.
[54] Desai SA, Patel VP, Bhosle KP, Nagare SD and Thombare KC. The tumor microenvironment: shaping cancer progression and treatment response. J Chemother 2025; 37: 15-44.
[55] Xu W, Li H, Hameed Y, Abdel-Maksoud MA, Almutairi SM, Mubarak A, Aufy M, Alturaiki W, Alshalani AJ, Mahmoud AM and Li C. Elucidating the clinical and immunological value of m6A regulator-mediated methylation modification patterns in adrenocortical carcinoma. Oncol Res 2023; 31: 819-831.
[56] Wang S, Yang J, You L, Dai M and Zhao Y. GSTM3 function and polymorphism in cancer: emerging but promising. Cancer Manag Res 2020; 12: 10377-10388.
[57] Chen T, Jinlin D, Wang F, Yuan Z, Xue J, Lu T, Huang W, Liu Y and Zhang Y. GSTM3 deficiency impedes DNA mismatch repair to promote gastric tumorigenesis via CAND1/NRF2-KEAP1 signaling. Cancer Lett 2022; 538: 215692.
[58] Gao Q, Ye X and Li F. SLC12A3: a novel prognostic biomarker of clear cell renal cell carcinoma. Altern Ther Health Med 2024; 30: 286-293.
[59] Li J, Li X, Zhang C, Zhang C and Wang H. A signature of tumor immune microenvironment genes associated with the prognosis of non-small cell lung cancer. Oncol Rep 2020; 43: 795-806.

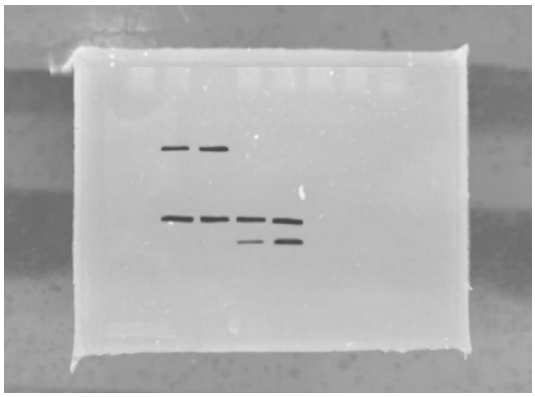

Figure S1. Uncut Western blot bands of SLC12A3, GSTM3 and GAPDH.